

Design, synthesis, and pharmacological evaluation of new neuroactive pyrazolo[3,4-*b*]pyrrolo[3,4-*d*]pyridine derivatives with in vivo hypnotic and analgesic profile

Ricardo Menegatti,^{a,b} Gilberto M. S. Silva,^{a,c} Gisele Zapata-Sudo,^c Juliana M. Raimundo,^c Roberto T. Sudo,^c Eliezer J. Barreiro^{a,b} and Carlos A. M. Fraga^{a,b,*}

^aLaboratory of Evaluation and Synthesis of Bioactive Substances (LASSBio), Faculdade de Farmácia, Universidade Federal do Rio de Janeiro, PO Box 68023, Rio de Janeiro 21944-971, RJ, Brazil

^bInstituto de Química, Universidade Federal do Rio de Janeiro, Rio de Janeiro 21949-900, RJ, Brazil

^cDepartamento de Farmacologia Básica e Clínica, Instituto de Ciências Biomédicas, Universidade Federal do Rio de Janeiro, Rio de Janeiro 21949-900, RJ, Brazil

Received 19 July 2005; revised 20 August 2005; accepted 22 August 2005

Available online 27 September 2005

Abstract—The present study describes the synthesis and pharmacological profiles of four novel pyrazolo[3,4-*b*]pyrrolo[3,4-*d*]pyridine derivatives **2–5**, which were structurally designed by using the sedative and analgesic drug zolpidem **1** as lead compound. The heterotricyclic system present in the target compounds **2–5** was constructed in good yields, exploiting a regioselective hetero Diels–Alder reaction of the key azabutadiene derivative **7** and functionalized *N*-phenylmaleimides **9–12**. Additionally, we identified that 1-methyl-7-(4-nitrophenyl)-3-phenyl-3,6,7,8-tetrahydropyrazolo[3,4-*b*]pyrrolo[3,4-*d*]pyridine-6,8-dione derivative (LASSBio-873, **5**) presented not only the most potent ability to promote sedation, which was similar to that induced by the standard benzodiazepine drug midazolam, but also potent central antinociceptive effect.

© 2005 Elsevier Ltd. All rights reserved.

1. Introduction

According to the US National Institute of Mental Health anxiety disorders affect annually more than 19 million adults ranging in age from 18 to 54 years, which represents 13.3% of the population at this age,¹ making this an important social problem of the contemporary world.

Zolpidem **1** (Fig. 1), an imidazo[1,2-*a*]pyridine derivative² with the ability to act as a benzodiazepine receptor agonist, is commonly used to treat anxiety disorders related to the neuronal inhibition induced by γ -aminobutyric acid (GABA),^{3,4} the major inhibitory neurotransmitter in the mammalian central nervous system (CNS).⁴ Drugs like **1** act through high potent and selec-

tive allosteric modulation of GABA_A receptors⁴ responsible for the regulation of the neuronal membrane conductance to chloride ions, promoting slight membrane hyperpolarization and a reduction in neuronal excitability.⁵ Similar processes are controlled by the opioid neurotransmission, in which the reduced neuronal excitability is translated in an analgesic effect.⁵ Recently, some reports demonstrated that analgesia and hyperalgesia are related to GABA-mediated modulation of the cerebral cortex.⁶

In the scope of a research program aimed at the development of new alternatives to treat neurological disorders, we describe in the present study the synthesis and pharmacological evaluation of new functionalized pyrazolo[3,4-*b*]pyrrolo[3,4-*d*]pyridine derivatives **2–5** (Fig. 1). These new heterotricyclic compounds were originally designed to be selective GABA receptor modulators, exploring its structural analogy with the lead compound zolpidem (**1**), which presents rapid-onset, short duration of hypnotic effect as a consequence of its binding to benzodiazepine receptors.^{2,7} Additionally, recent reports

Keywords: Hetero Diels–Alder reaction; Pyrazolo[3,4-*b*]pyrrolo[3,4-*d*]pyridine-6,8-dione; Hypnotic activity; Sedative properties; Central analgesic activity; Zolpidem analogues.

* Corresponding author. Tel.: +55 21 25626503; fax: +55 21 25626644; e-mail: cmfraga@pharma.ufrj.br

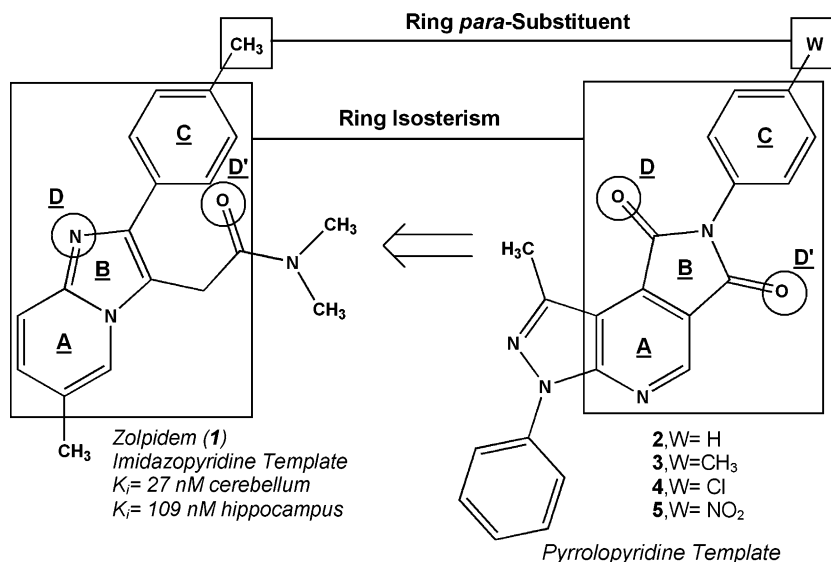


Figure 1. Design concept of the new heterotricyclic pyrazolo[3,4-*b*]pyrrolo[3,4-*d*]pyridine derivatives **2–5**.

have described that zolpidem (**1**) also has important analgesic properties, which seem to be dependent on a mechanism still unknown.^{8,9}

The title compounds **2–5** were structurally planned by exploring the isosteric relationship between the functionalized pyrrolo[3,4-*c*]pyridine-1,3-dione ring and the imidazo[1,2-*a*]pyridine moiety (**A** + **B**, Fig. 1) present in the lead compound **1**. Additionally, besides the maintenance of the corresponding substituted 2-phenyl group attached to the main heterocyclic template (**C**, Fig. 1), we promoted a second isosteric replacement of the two potential H-bond acceptor sites **D** and **D'** of **1**, by the two carbonyl groups of the pyrrolo-1,3-dione ring (**B**) present in the newly designed compounds **2–5** (Fig. 1). Focusing on its better CNS access, we decided to incorporate a *N*-phenylpyrazole framework to the bicyclic pyrrolo[3,4-*c*]pyridine-1,3-dione template, in order to improve the lipophilic behaviour of the new heterocyclic derivatives **2–5**, within the limits anticipated by Lipinski's rules.¹⁰

Aiming at the structural validation of the planned compounds **2–5**, we briefly evaluated the fit in the receptor site by using a new comparative molecular field analysis (CoMFA)¹¹ model for benzodiazepine (BZDP) ligands, which was constructed from a database containing a series of 58 (a training set of 46 and a test set of 12) known GABA_A/BZDP bioreceptor ligands described previously.^{12,13} The CoMFA model explored herein (see Fig. 2 and Table 1) was generated with a basis in the alignment anticipated in our previous LIV/3D-QSAR study,¹² applying the same set of BZDP ligands.

The CoMFA model was efficiently able to predict the activities of the compounds of the test set, suggesting that it can be used for the evaluation of new GABA_A/BzR ligand candidates, as well as the new pyrazolo[3,4-*b*]pyrrolo[3,4-*d*]pyridine derivatives **2–5**, which after

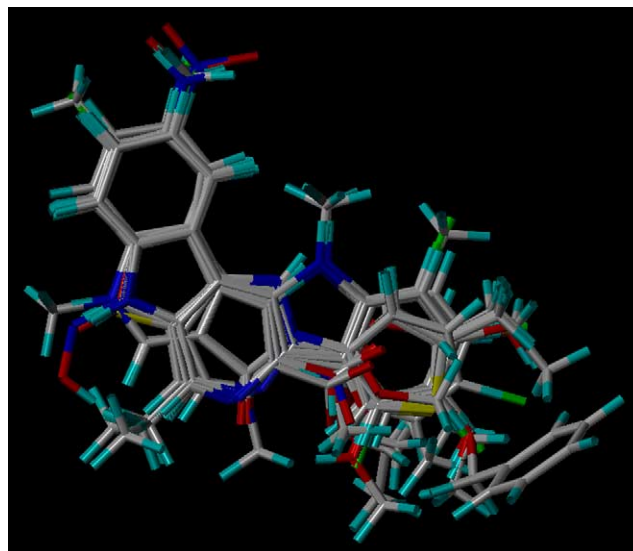


Figure 2. Superimposition and final alignment of the benzodiazepine ligands used in the generation of the corresponding CoMFA model.

Table 1. Statistical results for the new CoMFA model generated from the alignment of benzodiazepine ligands¹²

CoMFA model	
q^{2a}	0.841
N^b	6
S_{cv}^c	0.365
r^{2d}	0.941
S^e	0.305
F^f	104,097
r^2 pred ^g	0.871

^a Cross-validation correlation coefficient.

^b Number of components.

^c Standard error of prediction.

^d Correlation coefficient.

^e Standard error of estimate.

^f *F*-ratio.

^g Predicted correlation coefficient.

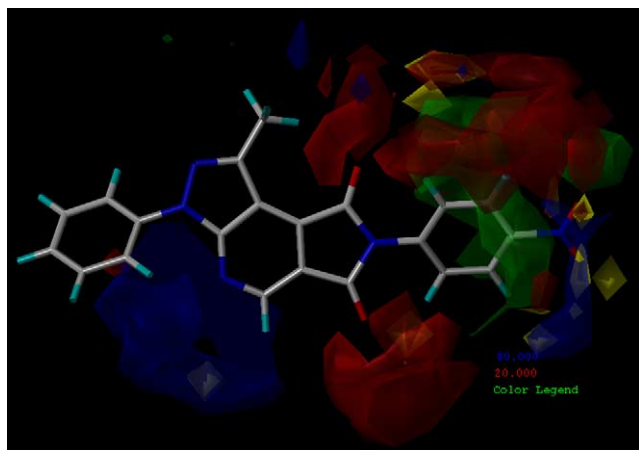


Figure 3. Contour maps of CoMFA model as compared with the topology of derivative **5**. The structures of the ligand are represented as sticks, highlighting the atoms in gray (C), blue (N), red (O), and light blue (H). Electrostatic contour plots of **5** are displayed in blue contours (>80% contribution) and red contours (<20% contribution), which correspond to regions where an increase in positive or negative charge, respectively, could enhance the bioactivity. Steric contour plots of **5** are displayed in green contours (>80% contribution) and yellow contours (<20% contribution), which indicate, respectively, regions where an increase in steric bulk could enhance or reduce the bioactivity.

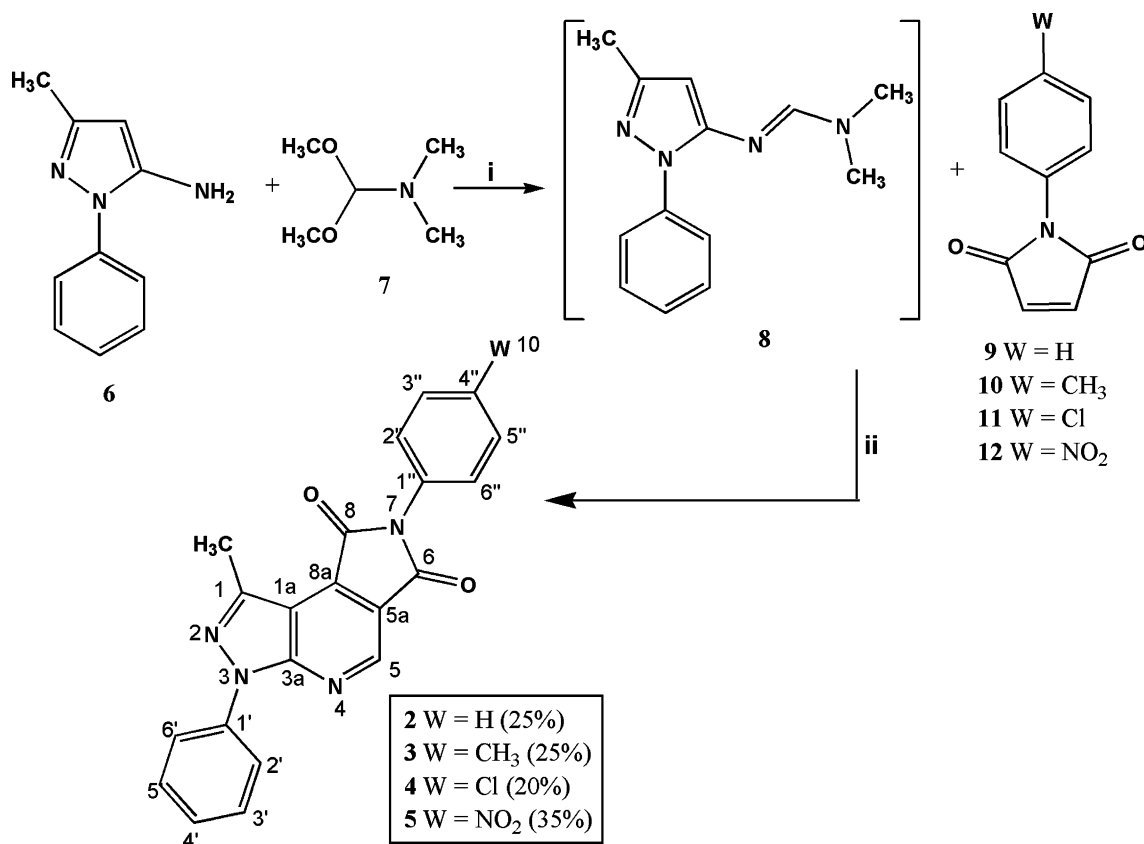
fitting presented predicted pIC_{50} values of 5.77, 6.08, 5.31, and 7.88 μM , respectively. The observed *in silico* profile corroborated the structural design of the new

class of heterotricyclic CNS agent candidates described herein, encouraging us to synthesize them (Fig. 3).

2. Chemistry

The synthetic route planned to achieve new heterotricyclic derivatives **2–5** (Scheme 1) exploited the use of hetero Diels–Alder reaction between the 2-azabutadiene intermediate **8** and substituted *N*-phenylmaleimides **9–12**, in acetic acid for 48 h.¹⁴ The 1-phenyl-3-methyl-5-aminopyrazole derivative **6** reagent was prepared according to the methodology previously described by Ganesan and Heathcock,¹⁵ which involves the coupling of β -aminocrotononitrile and phenylhydrazine. On the other hand, the (*E*)-2-azabutadiene derivative **8** was quantitatively prepared through the condensation reaction between **6** and dimethylformamide dimethylacetal **7**. Finally, the ene-moiety represented by substituted *N*-phenylmaleimide derivatives **9–12** was prepared in 60–75% yield, exploring the nucleophilic substitution of the maleic anhydride by the corresponding substituted aniline derivatives, according to the procedure described by Cava et al.¹⁶

For instance, the optimization of the hetero Diels–Alder step yields could be reached through the employment of non-acidic conditions.¹⁷ All new heterotricyclic derivatives described herein were completely characterized by common spectroscopic methods (see Experimental



Scheme 1. Reagents and conditions: (i) 90 °C, 6 h; (ii) AcOH, 50 °C, 48 h.

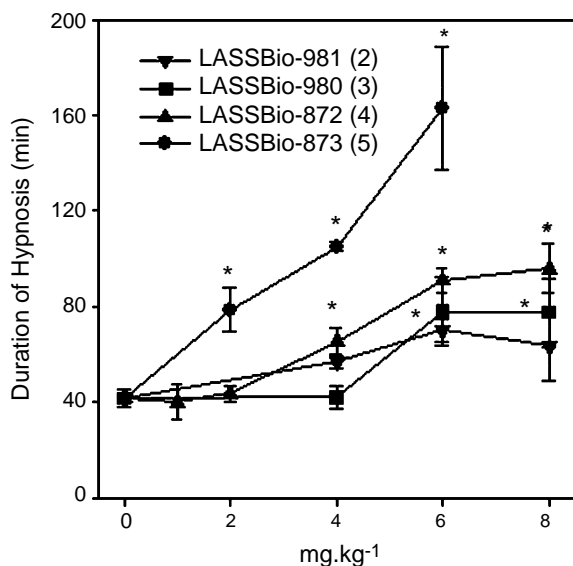


Figure 4. Effects of the new heterotricyclic compounds on the pentobarbital-induced sleep test.¹⁸ Derivatives were injected ip 30 min before intravenous injection of 25 mg kg⁻¹ of pentobarbital sodium. Data represent means of time between loss and recovery of the righting reflex. **P* < 0.05 relative to DMSO-treated group.

section) and their analytical results for C, H, and N were within ±0.4% of calculated values.

3. Pharmacology

The hypnotic effect of the title derivatives **2–5**, named, respectively, LASSBio-981, LASSBio-980, LASSBio-872, and LASSBio-873, was initially investigated by using the pentobarbital-induced-sleep test.¹⁸ All four new heterotricyclic derivatives increased the duration of hypnosis induced by pentobarbital in a dose-dependent manner (Fig. 4). The compounds **2**, **3**, **4**, and **5** in a dose of 6 mg kg⁻¹ significantly increased the pentobarbital-induced sleep from 41.7 ± 3.5 min (DMSO) to 70.1 ± 4.8, 78.0 ± 14.5, 98.7 ± 5.1, and 162.7 ± 25.8 min, respectively. The nitro-substituted derivative LASSBio-873 (**5**) was the most effective in prolonging

the duration of hypnosis induced by pentobarbital. These results indicated, as anticipated by the molecular modelling studies, that the inclusion of the NO₂ substituent in the heterotricyclic template favoured the efficacy of the compound in prolonging the pentobarbital effect.

Additionally, the sedation produced by the target derivatives **2–5** was investigated using the locomotor activity test.¹⁹ By applying this in vivo protocol we could evidence that, excepting the derivative **3**, all substituted pyrazolo[3,4-*b*]pyrrolo[3,4-*d*]pyridine derivatives (e.g., **2**, **4**, and **5**) significantly altered the spontaneous locomotor activity (Fig. 5). Intraperitoneal injection of derivatives **2** (6 mg kg⁻¹), **4** (6 mg kg⁻¹) and **5** (4 mg kg⁻¹) decreased motor activity from 209.1 ± 26.2 movements/min (DMSO) to 93.7 ± 15.2, 129.6 ± 22.7 and 86.7 ± 16.5 movements/min, respectively. The reduction in locomotor activity was comparable to that of the reference agent midazolam,²⁰ which in a dose of 2 mg kg⁻¹ was able to decrease motor activity to 80.9 ± 26.6 movements/min (Fig. 5). Once again, compound LASSBio-873 (**5**) presented the most potent sedative effect in comparison with the other heterotricyclic derivatives **2–4**.

Considering the described analgesic profile exhibited by the non-benzodiazepine hypnotic drug zolpidem⁹ (**1**), which could be evidenced only in high doses, i.e., 80 mg kg⁻¹ (sc), promotes 80% of analgesia in mice, we decided to investigate the central antinociceptive profile of the designed heterocyclic derivatives **2–5** in the same experimental protocol, i.e., hot plate test.²¹ As shown in Figure 6, a single intraperitoneal administration of the target compounds **2**, **3**, **4**, and **5** resulted in a remarkable analgesic effect. The analgesic activity was dose dependent for all new pyrazolo[3,4-*b*]pyrrolo[3,4-*d*]pyridine derivatives described herein. Maximal analgesic activity (100%) was observed with the compounds LASSBio-872 (**4**) (6 mg kg⁻¹) and LASSBio-873 (**5**) (2 mg kg⁻¹). Therefore, nitro-substituted derivative **5** was the most potent to produce analgesia and the duration of its action was greater than 2 h. After 30 min of an intraperitoneal injection of 4 mg kg⁻¹, analgesic activity evidenced for derivatives **2–5** was 61.9 ± 16.2,

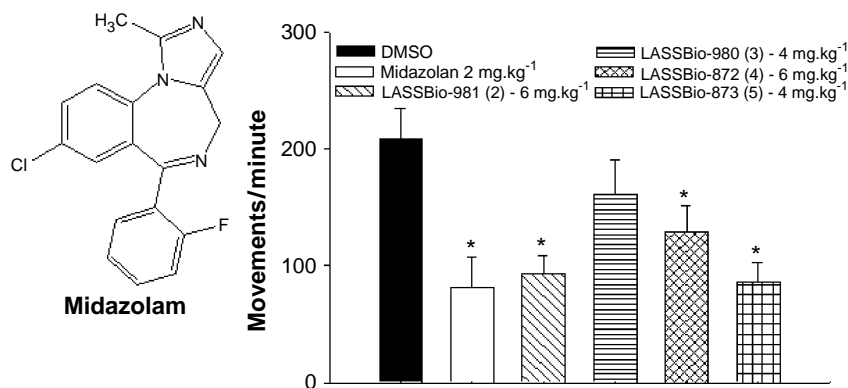


Figure 5. Effects of midazolam and new heterotricyclic compounds on the locomotor activity in mice.¹⁹ Derivatives were injected ip and motor activity was determined during 40 min after injection. Data are expressed as means of the movements per minute ± SEM. **P* < 0.05 relative to control group (DMSO).

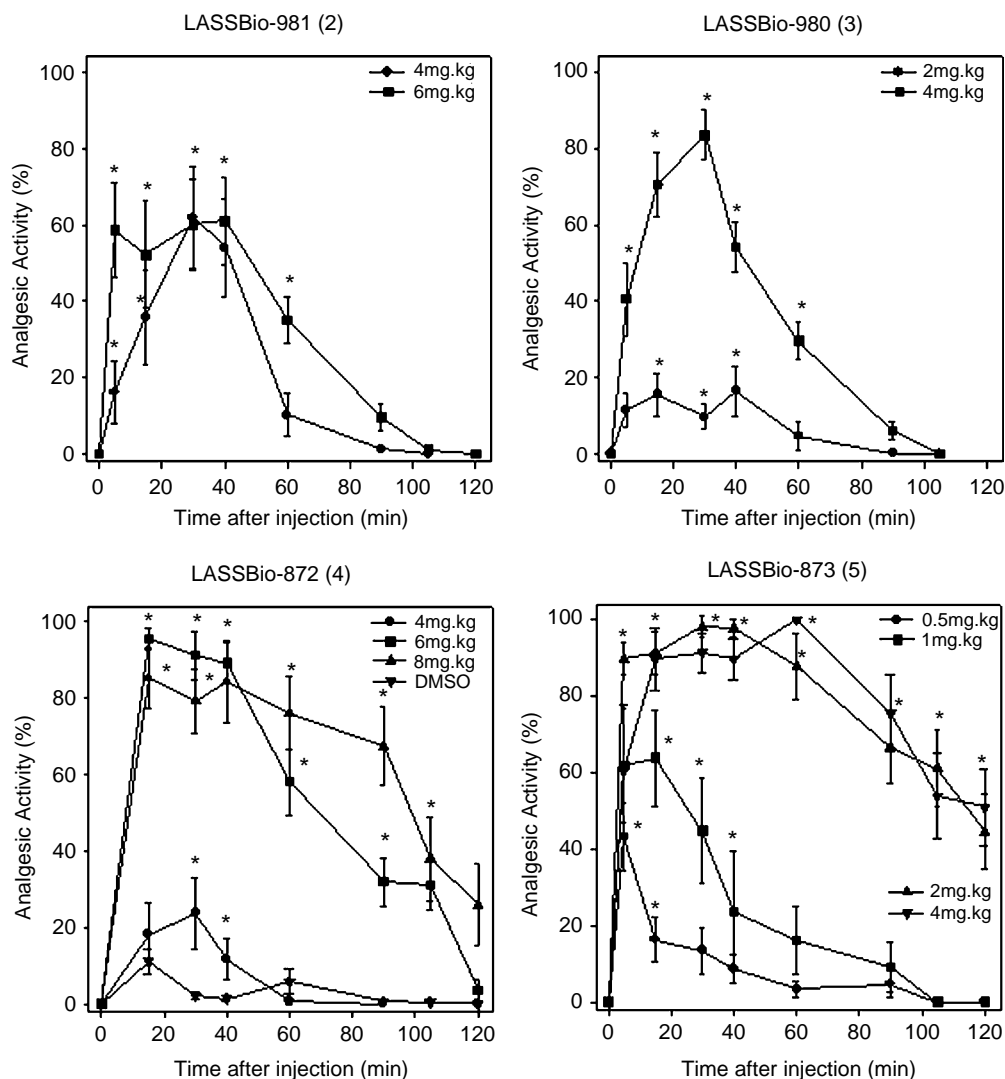


Figure 6. Effects of the new heterotricyclic derivatives **2–5** on the thermal stimuli response using the hot plate test.²¹ Derivatives were injected ip in mice. Data are expressed as means of the percentage of analgesic activity considering the cutoff of 35 s. * $P < 0.05$ relative to control group at a given time.

83.5 ± 6.5 , 23.7 ± 9.2 , and $91.3 \pm 5.0\%$, respectively (Fig. 6). Dose-antinociceptive response curves induced by heterotricyclic derivatives **2–5** were evaluated in the presence of naloxone, an antagonist of opioid receptors.²² Treatment of mice with naloxone (1 mg kg^{-1}) before the ip administration of all new derivatives tested reduced its analgesic activity (Fig. 7), indicating that this bioprofile seems to be dependent on the activation of opioid receptors.

These results showed that unlike zolpidem (**1**), which presents a weak antinociceptive profile in doses far beyond those used clinically to induce sleep,⁹ the nitro-heterotricyclic derivative LASSBio-873 (**5**) has a powerful analgesic profile in doses two times lower than that able to induce a midazolam-like sedative effect.

In conclusion, we discovered a new potent central acting analgesic prototype represented by compound LASSBio-873 (**5**), which was structurally designed from

benzodiazepine receptor ligand zolpidem (**1**) through the identification of the bioisosteric relationships between imidazo[1,2-*a*]pyridine and pyrrolo[3,4-*c*]pyridine-1,3-dione heterocyclic frameworks. In addition, as previously evidenced for the analgesic activity of zolpidem (**1**), the antinociceptive profile of LASSBio-873 (**5**) seems to be directly or indirectly dependent on the modulation of opioid receptors.

4. Experimental

4.1. Generation of benzodiazepine CoMFA model

4.1.1. Biological data. Based on the previous study,¹² we selected a series of 58 non-benzodiazepine compounds in which their ability to replace the [^3H]diazepam on the specific binding assay for the GABA_A/benzodiazepine receptor was used as a parameter for the evaluation of the biological activity.¹³ The binding affinities measured as IC_{50} (nM) were converted to IC_{50} (M) and then

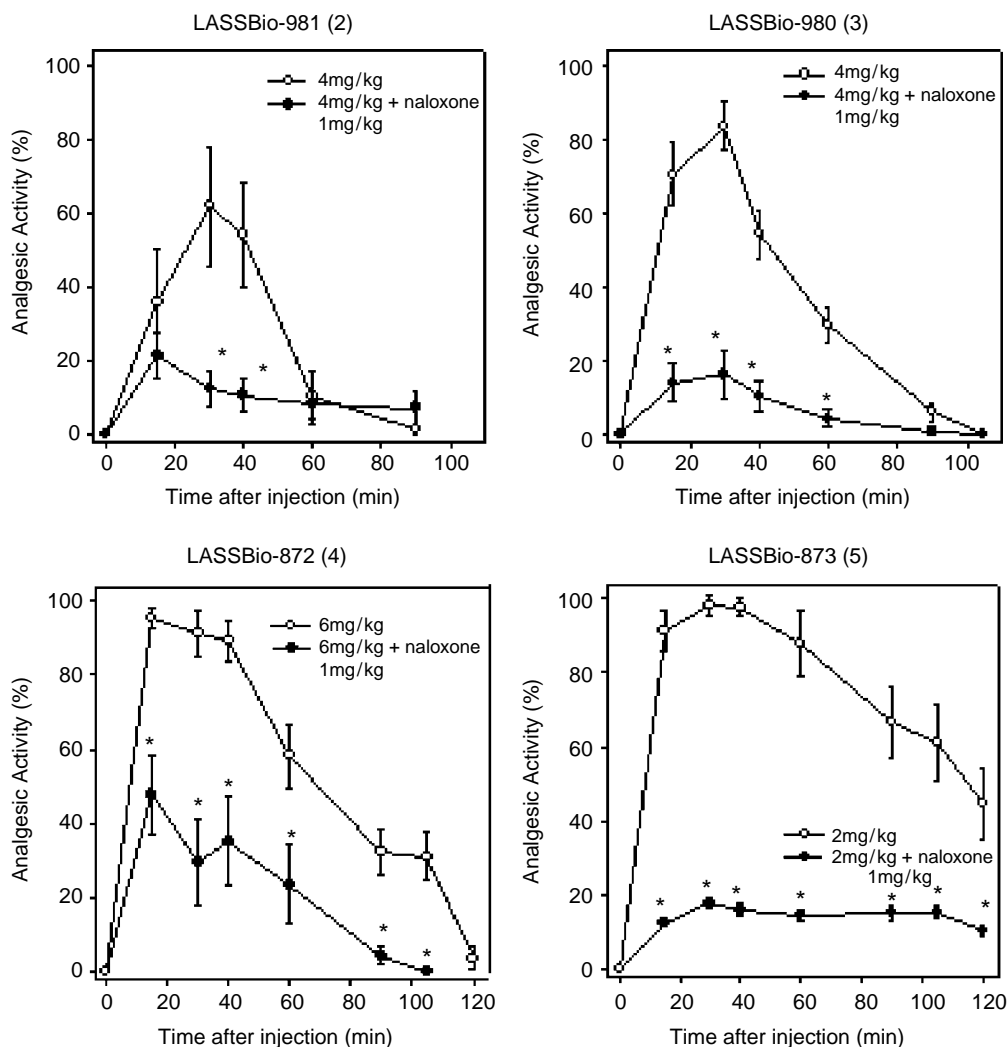


Figure 7. Effects of the new heterotricyclic derivatives **2–5** on the thermal stimuli response using the hot plate test in the absence and presence of naloxone. Derivatives were injected ip in mice 15 min after pre-treatment with naloxone (1 mg kg^{-1}). Data are expressed as means of the percentage of analgesic activity considering the cutoff of 35 s. * $P < 0.05$ relative to group treated with derivatives alone at a given time.

converted to pIC_{50} , and those expressed as K_i (nM) were first converted to IC_{50} (M) according to the Cheng and Prusoff equation.²³ The binding affinities were widespread and homogeneous, which is an important requisite to the obtainment of meaningful results from 3D-QSAR studies using the CoMFA method.²⁴ Approximately 80% of the 58 compounds were selected to compose the training set (46 compounds) and the remaining compounds, corresponding to approximately 20%, were used as test set (12 compounds). The compounds were split between training and test sets at random. Random numbers were generated and assigned to each compound before they were sorted in increasing order. Then the training set was used as the basis to construct the CoMFA model and the compounds of the test set were used for model validation.

4.1.2. Molecular modelling and alignment. The initial structures of the 58 non-benzodiazepine compounds were generated by application of semiempirical AM1 minimization according to previous report by our research group.¹² The geometries of these compounds

were subsequently optimized using the Tripos force field with Gasteiger–Hückel charges. The Powell method available in the Maximin2 module of Sybyl 7.0²⁵ was used for energy minimization with an energy convergence gradient value of $0.001 \text{ kcal/(mol \AA)}$. Additionally, previous alignment¹² was used for superposition of all 58 GABA_A/BZDP bioreceptor ligands. The illustration of this alignment is presented in Figure 2.²⁶

4.1.3. 3D QSAR/CoMFA analysis. The CoMFA method was applied to the training set for the 3D QSAR analysis. The steric (Lennard–Jones) and electrostatic (Coulomb) CoMFA fields were calculated at all intersections in a regularly spaced (1.5 \AA) grid within a predefined region. The steric and electrostatic interaction energies between a probe atom and the molecules were calculated using a sp^3 carbon as the steric probe atom and a $+1.00$ charge for the electrostatic probe. A cutoff of 5 kcal/mol was adopted, and the regression analysis was carried out using the full cross-validated partial least-squares (PLS)^{27,28} method (leave-one-out) with CoMFA standard options for scaling of variables.

To perform the PLS, the minimum column filtering value was set to 4.0 kcal/mol to improve the signal-to-noise ratio by omitting those lattice points whose energy variation was below this threshold and the number of components was set to 5.

4.2. Chemistry

All melting points were determined with a Thomas–Hoover apparatus and are uncorrected. Proton magnetic resonance (^1H NMR), unless otherwise stated, was determined in deuterated chloroform containing ca. 1% tetramethylsilane as an internal standard with Bruker 500 MHz. Splitting patterns are as follows: s, singlet; d, doublet; dd, double doublet; m, multiplet. Carbon magnetic resonance (^{13}C NMR) was determined with the same spectrometer described above at 125 MHz. Infrared (IR) spectra were obtained with a Nicolet-55a Magna spectrophotometer by using potassium bromide plates. The ultraviolet spectra were obtained with a Hitachi U-2000 Spectrophotometer by using methanol as solvent and an internal standard. Microanalysis data were obtained with a Perkin-Elmer 240 analyzer, using Perkin-Elmer AD-4 balance.

The progress of all reactions was monitored by TLC, which was performed on 2.0×6.0 cm aluminium sheets precoated with silica gel 60 (HF-254, Merck) to a thickness of 0.25 mm. The developed chromatograms were viewed under ultraviolet light (254–265 nm) and treated with iodine vapour. For column chromatography Merck silica gel (70–230 mesh) was used. Reagents and solvents were purchased from commercial suppliers and distilled prior the use.

4.2.1. General procedure¹⁴ for the ‘one-pot’ preparation of the heterotricyclic derivatives LASSBio-981 (2), LASSBio-980 (3), LASSBio-872 (4), and LASSBio-873 (5). A mixture of 1-phenyl-3-methyl-5-aminopyrazole¹⁵ (2.5 mmol) and dimethylformamide dimethylacetal (2.75 mmol) was heated at 90 °C for 6 h. Then, the resulting aggregate was dissolved in acetic acid (10 mL), followed by the addition of the corresponding substituted *N*-phenylmaleimide¹⁶ **9–12** (10.0 mmol). The suspension was stirred vigorously and heated at 50 °C for an additional 48 h. After cooling at room temperature, the reaction mixture was poured in water (20 mL), filtered, and rinsed with ethanol to afford the desired heterotricyclic derivative **2–5** as described next.

4.2.2. 7-Phenyl-1-methyl-3-phenyl-3,6,7,8-tetrahydropyrazolo[3,4-*b*]pyrrolo[3,4-*d*]pyridine-6,8-dione, LASSBio-981 (2). Derivative **2** was obtained in 25% yield, as a yellow solid, mp 228–230 °C, $R_f = 0.84$ ($\text{CH}_2\text{Cl}_2/\text{MeOH}$ 95:5) and $R_f = 0.79$ (*n*-hexane/ethyl acetate 7:3); IR_{max} (KBr) cm^{-1} : 3112–3055 (νC–H), 1779–1717 (νC=O); ^1H NMR (500 MHz) CDCl_3/TMS (δ —ppm): 9.07 (1H, s, H-9), 8.14 (2H, d, $J = 8.0$ Hz, H-2'' and 6''), 7.51–7.47 (4H, m, 3', 5', 2'' and 6''), 7.41–7.37 (3H, m, 3'', 4'' and 5''), 7.32 (1H, d, $J = 7.5$ Hz, H-4'), 2.90 (3H, s, Me); ^{13}C NMR (125 MHz) CDCl_3/TMS (δ —ppm): 166.7 and 165.6 (C-8 and C-7), 153.6 (C-5), 143.9 (C-1), 143.7 (C-3a), 138.5 (C-1'), 134.7 (C-8a), 131.2 (C-

1''), 129.3 (C-3', 5', 2'' and 6''), 128.5 (C-4''), 127.1 (C-4'), 126.6 (C-3'' and 5''), 121.8 (C-2' and 6'), 119.5 (C-5a), 110.7 (C-1a); 15.1 (Me); UV $\lambda_{\text{max}}^{(\text{CHCl}_3)}$ nm (ϵ_{MAX}): 386.2 (1330); 283.6 (36,702).

4.2.3. 7-(4-Methylphenyl)-1-methyl-3-phenyl-3,6,7,8-tetrahydropyrazolo[3,4-*b*]pyrrolo[3,4-*d*]pyridine-6,8-dione, LASSBio-980 (3). Derivative **3** was obtained in 25% yield, as a yellow solid, mp 231–233 °C, $R_f = 0.84$ ($\text{CH}_2\text{Cl}_2/\text{MeOH}$ 95:5) and $R_f = 0.80$ (*n*-hexane/ethyl acetate 7:3); IR_{max} (KBr) cm^{-1} : 3111–3041 (νC–H); 2920–2845 (νC–H); 1778–1720 (νC=O); ^1H NMR (500 MHz) CDCl_3/TMS (δ —ppm): 9.04 (1H, s, H-5), 8.13 (2H, d, $J = 8.5$ Hz, H-2'' and 6''), 7.48 (2H, t, $J = 8.0$ Hz, H-3' and 5'), 7.25–7.31 (5H, m, H-2', 4', 6', 3'' and 5''), 2.88 (3H, s, H-9), 2.36 (3H, s, H-10); ^{13}C NMR (125 MHz) CDCl_3/TMS (δ —ppm): 166.8 (C-8), 165.7 (C-6), 153.6 (C-1), 143.9 (C-5), 143.7 (C-3a), 138.7 (C-1'), 138.5 (C-1''), 134.7 (C-8a), 129.9 (C-3' and 5'), 129.2 (C-2'' and 6''), 128.5 (C-4''), 127.0 (C-4'), 126.4 (C-3'' and 5''), 121.8 (C-2' and 6'), 119.6 (C-5a), 110.7 (C-8a), 21.3 (C-10), 15.1 (Me); UV $\lambda_{\text{max}}^{(\text{CHCl}_3)}$ nm (ϵ_{MAX}): 386.2 (1215); 285.2 (33,094).

4.2.4. 7-(4-Chlorophenyl)-1-methyl-3-phenyl-3,6,7,8-tetrahydropyrazolo[3,4-*b*]pyrrolo[3,4-*d*]pyridine-6,8-dione, LASSBio-872 (4). Derivative **4** was obtained in 20% yield, as a yellow solid, mp 246–248 °C, $R_f = 0.87$ ($\text{CH}_2\text{Cl}_2/\text{MeOH}$ 95:5) and $R_f = 0.64$ (*n*-hexane/ethyl acetate 7:3); IR_{max} (KBr) cm^{-1} : 3092–3072 (νC–H), 1774–1726 (νC=O), 1092 (νC–Cl); ^1H NMR (500 MHz) CDCl_3/TMS (δ —ppm): 9.08 (1H, s, H-5), 8.14 (2H, d, $J = 8.0$ Hz, H-2' and 6'), 7.50 (2H, t, $J = 8.0$ Hz, H-3' and 5'), 7.46 (2H, d, $J = 8.2$ Hz, H-2'' and 6''), 7.38 (2H, d, $J = 8.2$ Hz, H-3'' and 5''), 7.32 (1H, t, $J = 8.0$ Hz, H-4'), 2.90 (3H, s, H-9); ^{13}C NMR (125 MHz) CDCl_3/TMS (δ —ppm): 166.3 (C-8), 165.3 (C-6), 153.7 (C-1), 143.9 (C-5), 143.6 (C-3a), 138.5 (C-1'), 134.5 (C-8a), 134.3 (C-1''), 129.7 (C-4''), 129.5 (C-2'' and 6''), 129.2 (C-3' and 5'), 127.7 (C-3'' and 5''), 127.1 (C-4'), 121.9 (C-2' and 6'), 119.3 (C-5a), 110.7 (C-1a), 15.1 (Me); UV $\lambda_{\text{max}}^{(\text{CHCl}_3)}$ nm (ϵ_{MAX}): 386.2 (1220); 285.6 (34,476).

4.2.5. 1-Methyl-7-(4-nitrophenyl)-3-phenyl-3,6,7,8-tetrahydropyrazolo[3,4-*b*]pyrrolo[3,4-*d*]pyridine-6,8-dione, LASSBio-873 (5). Derivative **5** was obtained in 35% yield, as a yellow solid, mp 238–240 °C, $R_f = 0.87$ ($\text{CH}_2\text{Cl}_2/\text{MeOH}$ 95:5) and $R_f = 0.56$ (*n*-hexane/ethyl acetate 7:3); IR_{max} (KBr) cm^{-1} : 3124–3004 (νC–H), 1727 (νC=O), 1350–1380 (νC–NO₂), 848–884 (νC–NO₂); ^1H NMR (500 MHz) CDCl_3/TMS (δ —ppm): 9.12 (1H, s, H-5), 8.36 (2H, d, $J = 9.0$ Hz, H-3'' and 5''), 8.15 (2H, d, $J = 8.0$ Hz, H-2' and 6'), 7.74 (2H, d, $J = 9.0$ Hz, H-2'' and 6''), 7.51 (2H, t, $J = 8.0$ Hz, H-3' and 5'), 7.34 (1H, t, $J = 8.0$ Hz, H-4'), 2.92 (3H, s, H-9); ^{13}C NMR (500 MHz) CDCl_3/TMS (δ —ppm): 166.8 (C-8), 165.8 (C-6), 153.8 (C-1), 146.6 (C-4''), 144.2 (C-5), 143.8 (C-3a), 138.3 (C-1'), 137.1 (C-1''), 134.2 (C-8a), 129.3 (C-3' and 5'), 127.3 (C-4'), 126.5 (C-2'' and 6''), 124.6 (C-3'' and 5''), 121.9 (C-2' and 6'), 119.0 (C-5a), 110.7 (C-1a), 15.1 (Me); UV $\lambda_{\text{max}}^{(\text{CHCl}_3)}$ nm (ϵ_{MAX}): 386.2 (1377); 293.0 (34,970).

4.3. Pharmacology

The Animal Care and Use Committee at Universidade Federal do Rio de Janeiro approved the protocols described as follows.

4.3.1. Pentobarbital-induced sleep test in mice.¹⁸ Male Swiss mice (20–25 g) were randomly divided into groups of 10 and housed in a breeding room with 12 h light–dark cycle at 24 ± 1 °C. Each group was ip injected with each derivative LASSBio-872 (**2**), LASSBio-873 (**3**), LASSBio-980 (**4**), and LASSBio-981 (**5**) 30 min before intravenous administration of pentobarbital sodium (25 mg kg⁻¹). Doses of the heterotricyclic derivatives varied from 1 to 8 mg kg⁻¹. Sleep time was considered as the difference between the time of loss and recovery of the righting reflex. The compounds **2–5** were dissolved in dimethylsulfoxide (DMSO) as stock solutions of 50 mg/mL. Control group was ip treated with DMSO alone to determine the duration of hypnosis.

4.3.2. Locomotor activity test in mice.¹⁹ The sedative properties of midazolam and derivatives were compared using locomotor activity as an index of sedation. Motor activity was determined in Swiss mice (20–25 g), which were placed in an open field of 45 × 45 cm (LE 8811, Leticia) in which 16 photocell beams were positioned every 2.5 cm. Total locomotor activity was defined as the number of interruptions of the beams registered in a computer. Activity was measured during 40 min after ip injection of either midazolam or new heterotricyclic derivatives **2–5**.

4.3.3. Antinociceptive activity (hot plate test).²¹ Central analgesic activity was evaluated using the method of hot plate. One hundred and twenty male Swiss mice (20–25 g) were randomly divided into 12 groups and each group of 10 mice was treated with vehicle (DMSO) alone or with different doses of heterotricyclic derivatives **2–5**, varying from 0.5 to 8 mg kg⁻¹. Mice were placed into a hot plate maintained at 52 °C (Leticia LE 7406). The time necessary for each animal to respond to the termic stimuli was determined before and after pre-treatment with the pyrazolo[3,4-*b*]pyrrolo[3,4-*d*]pyridine derivatives from 5 to 120 min after injection. Four groups of mice (*n* = 10 each) were pre-treated with ip injection of 1 mg kg⁻¹ of naloxone 15 min before the administration of test compounds **2–5**. Maximal permanence of the animals was 35 s (cutoff). Data were expressed in means ± SEM of analgesic activity. The analgesic activity (%) was calculated by the following equation:

$$\text{Analgesic Activity} = \frac{(\text{postdrug latency}) - (\text{predrug latency})}{(35 \text{ s}) - (\text{predrug latency})} \times 100$$

4.3.4. Statistical analysis. Statistical significance was assessed using one- or two-way analysis of variance (ANOVA) followed by a Student–Neuman–Keuls test. Difference was considered statistically significant when *P* < 0.05.

Acknowledgments

Thanks are due to CNPq (BR.), PRONEX (BR.), CAPES (BR.), FAPERJ (BR.) and FUJB (BR.) for financial support and fellowships (R.M., J.M.R., C.A.M.F., and E.J.B.). We also thank the analytical centers of NPPN-UFRJ (BR.) and Farmanguinhos-FIOCRUZ (BR.) for spectroscopic facilities.

Supplementary data

Supplementary data associated with this article can be found in the online version at doi:10.1016/j.bmc.2005.08.042

References and notes

1. <http://www.phrma.org>; Survey New Medicines in Development for Mental Illnesses, 2002: New Survey Finds 99 Medicines in Clinical Testing for Mental Illnesses, Pharmaceutical Research and Manufacturers of America (PHRMA), Washington, DC.
2. Sanger, D. J.; Depoortee, H. *CNS Drug Rev.* **1998**, *4*, 323–340.
3. Möhler, H.; Crestani, F.; Rudolph, U. *Curr. Opin. Pharmacol.* **2001**, *1*, 22–25.
4. Williams, D. A.; Lemke, T. L. *Foye's Principles of Medicinal Chemistry*, 5th ed.; Lippincott Williams & Wilkins: Philadelphia, 2002.
5. Hardman, J. G.; Limbird, L. E. *Goodman & Gilman's The Pharmacological Basis of Therapeutics*, 10th ed.; McGraw-Hill: New York, 2001.
6. Jasmin, L.; Rabkin, S. D.; Granato, A.; Boudah, A.; Ohara, P. T. *Nature* **2003**, *424*, 316–320.
7. Wagner, J.; Wagner, M. L. *Sleep Med. Rev.* **2000**, *4*, 551–581.
8. Zaks, A. *US Patent* **2004**, *204*, 443.
9. Pick, C. G.; Chernes, Y.; Rigai, T.; Rice, K. C.; Schreiber, S. *Pharmacol. Biochem. Behav.* **2005**, *81*, 417–423.
10. Lipinski, C. A. *Drug Discov. Today: Technol.* **2004**, *1*, 337–341.
11. Cramer, R. C.; Patterson, D. E.; Bunce, J. D. *J. Am. Chem. Soc.* **1988**, *110*, 5959–5967.
12. Verli, H.; Albuquerque, M. G.; Alencastro, R. B.; Barreiro, E. J. *Eur. J. Med. Chem.* **2002**, *37*, 219–229.
13. The chemical structure of all 58 derivatives employed in the construction of the benzodiazepine CoMFA model is described in the [supplementary data](#).
14. Mason, H. J.; Wu, X.; Schmitt, R.; Macor, J. A.; Yu, G. *Tetrahedron Lett.* **2001**, *42*, 8931–8934.
15. Ganesan, A.; Heathcock, C. H. *J. Org. Chem.* **1993**, *58*, 6155–6157.
16. Cava, M. P.; Deana, A. A.; Muth, K.; Mitchell, A. J. *Org. Synth. Coll.* **1973**, *5*, 944.
17. Illustratively after the solvent exchange from AcOH to DMSO the Diels–Alder reaction between the heterodiene **8** with phenylmaleimide **9** was able to produce in 75% yield the pyrazolo[3,4-*b*]pyrrolo[3,4-*d*]pyridine derivative **2**.
18. Tsuji, R.; Isobe, N.; Kawasaki, H. *Toxicology* **1996**, *108*, 185–190.
19. Mara, S.; Diaz-Veliz, G.; Lungenstrass, H.; Garcia-Gonzalez, M.; Coto-Morales, T.; Poletti, C.; De Lima, T. C. M.; Herrera-Ruiz, M.; Tortoriello, J. *J. Ethnopharmacol.* **2005**, *97*, 191–197.
20. Dundee, J. W.; Halliday, N. J.; Harper, K. W.; Brogden, R. N. *Drugs* **1984**, *28*, 519–543.

21. Kuraishi, Y.; Harada, Y.; Aratani, S.; Satoh, M.; Takagi, H. *Brain Res.* **1983**, 273, 245–252.
22. McNicholas, L. F.; Martin, W. R. *Drugs* **1984**, 27, 81–93.
23. Cheng, Y. C.; Prusoff, W. H. *Biochem. Pharmacol.* **1973**, 22, 3099–3108.
24. Kubinyi, H. In *QSAR: Hansch Analysis and Related Approaches. Methods and Principles in Medicinal Chemistry*; Mannhold, R., Krogsgaard-Larsen, P., Timmerman, H., Eds.; VHC: Weinheim, 1993.
25. Sybyl Version 7.0. Tripos Associates: St. Louis, MO, 2004.
26. The atoms used to fit the new heterotricyclic derivatives **2–5** in the CoMFA model were N4 C8 and C6=O (see [Scheme 1](#)).
27. Weiner, S. J.; Kollman, P. A.; Case, D. A.; Singh, C.; Ghio, G.; Alagona, S.; Profeta, P.; Weiner, P. J. *Am. Chem. Soc.* **1984**, 106, 765.
28. Ghose, A. K.; Viswanadhan, V. N.; Wendoloski, J. J. *J. Comb. Chem.* **1999**, 1, 55.